British Journal of Pharmacology (2006) 148, 61–69
www.nature.com/bjp

Biological properties of a specific $G\alpha_{q/11}$ inhibitor, YM-254890, on platelet functions and thrombus formation under high-shear stress

*,[1]Toshio Uemura, [1]Tomihisa Kawasaki, [1]Masatoshi Taniguchi, [1]Yumiko Moritani, [1]Kazumi Hayashi, [1]Tetsu Saito, [1]Jun Takasaki, [1]Wataru Uchida & [1]Keiji Miyata

[1]Institute for Drug Discovery Research, Astellas Pharma Inc., 21 Miyukigaoka, Tsukuba, Ibaraki 305-8585, Japan

1 The effects of YM-254890, a specific $G\alpha_{q/11}$ inhibitor, on platelet functions, thrombus formation under high-shear rate condition and femoral artery thrombosis in cynomolgus monkeys were investigated.

2 YM-254890 concentration dependently inhibited ADP-induced intracellular Ca^{2+} elevation, with an IC_{50} value of $0.92 \pm 0.28\,\mu M$.

3 P-selectin expression induced by ADP or thrombin receptor agonist peptide (TRAP) was strongly inhibited by YM-254890, with IC_{50} values of 0.51 ± 0.02 and $0.16 \pm 0.08\,\mu M$, respectively.

4 YM-254890 had no effect on the binding of fibrinogen to purified GPIIb/IIIa, but strongly inhibited binding to TRAP-stimulated washed platelets.

5 YM-254890 completely inhibited platelet shape change induced by ADP, but not that induced by collagen, TRAP, arachidonic acid, U46619 or A23187.

6 YM-254890 attenuated ADP-, collagen-, TRAP-, arachidonic acid- and U46619-induced platelet aggregation with IC_{50} values of $<1\,\mu M$, whereas it had no effect on phorbol 12-myristate 13-acetate-, ristocetin-, thapsigargin- or A23187-induced platelet aggregation.

7 High-shear stress-induced platelet aggregation and platelet-rich thrombus formation on a collagen surface under high-shear flow conditions were concentration dependently inhibited by YM-254890.

8 The antithrombotic effect of YM-254890 was evaluated in a model of cyclic flow reductions in the femoral artery of cynomolgus monkeys. The intravenous bolus injection of YM-254890 dose dependently inhibited recurrent thrombosis without affecting systemic blood pressure or prolonging template bleeding time.

9 YM-254890 is a useful tool for investigating $G\alpha_{q/11}$-coupled receptor signaling and the physiological roles of $G\alpha_{q/11}$.
British Journal of Pharmacology (2006) **148,** 61–69. doi:10.1038/sj.bjp.0706711;
published online 6 March 2006

Keywords: a $G\alpha_{q/11}$ inhibitor; platelet aggregation; shape change; platelet activation; high-shear stress; thrombosis

Abbreviations: CFRs, cyclic flow reductions; FITC, fluorescein isothiocianate; PE, phycoerythrin; PerCP, perdinin chlorophyll protein; PMA, phorbol 12-myristate 13-acetate; PPP, platelet-poor plasma; PRP, platelet-rich plasma; SIPA, shear stress-induced platelet aggregation; TRAP, thrombin receptor agonist peptide

Introduction

Platelet activation plays a central role in hemostasis as well as in various thromboembolic diseases like unstable angina, myocardial infarction and stroke (Goldschmidt *et al*., 2002). Most platelet-activating stimuli function through receptors that couple to the heterotrimeric G proteins of the $G\alpha_i$, $G\alpha_q$ and $G\alpha_{12}$ families (Birnbaumer, 1992; Brass *et al*., 1993; Clapham & Neer, 1993). Recent studies have elucidated the roles of individual G proteins in the regulation of platelet functions like shape change, granule secretion and aggregation. The signaling pathways mediated by heterotrimeric G proteins operate synergistically to induce full platelet activation (Akkerman & van Willigen, 1996; Offermanns, 2000).

The crucial role of $G\alpha_q$ in platelet activation has been elucidated using platelets from a patient with decreased immunoreactive $G\alpha_q$ (Gabbeta *et al*., 1997) as well as from $G\alpha_q$-deficient mice (Offermanns *et al*., 1997). Clinical analysis of a patient suffering from a mild life-long mucocutaneous bleeding diathesis associated with prolonged bleeding time and normal platelet counts demonstrated diminished platelet aggregation and secretion in response to multiple agonists, despite the presence of normal dense granule stores. Immunoblot analysis of the $G\alpha_q$ subunits in this patient's platelet membranes showed a decrease in $G\alpha_q$ ($<50\%$), but not $G\alpha_i$, $G\alpha_z$, or $G\alpha_{12}$ and $G\alpha_{13}$ (Gabbeta *et al*., 1997). Similarly, platelets from $G\alpha_q$-deficient mice are unresponsive to a variety of physiological platelet agonists. As a result, $G\alpha_q$-deficient mice have increased bleeding times and are protected from collagen and adrenaline-induced thromboembolism (Offermanns *et al*., 1997). Thus, the possibility of $G\alpha_q$ as a new target for antiplatelet agents has been suggested, but no compound that inhibits $G\alpha_q$ has been reported so far.

YM-254890, which is a cyclic depsipeptide discovered in our laboratories from *Chromobacterium* sp. QS3666 culture broth,

*Author for correspondence; E-mail: toshio.uemura@jp.astellas.com

is a potent inhibitor of ADP-induced platelet aggregation (Taniguchi *et al*., 2003). Our recent studies demonstrated that YM-254890 selectively inhibited $G\alpha_{q/11}$, and the step at which it acts is when GDP changes to GTP during $G\alpha_{q/11}$ activation (Takasaki *et al*., 2004). The compound also exhibited antithrombotic and thrombolytic effects after i.v. bolus injection in an electrically induced carotid artery thrombosis model in rats (Kawasaki *et al*., 2003). However, the biological properties of YM-254890 on platelet functions and platelet thrombus formation under high-shear stress have not yet been reported.

In this study, we examined the biochemical properties of YM-254890 on platelet functions such as intracellular Ca^{2+} elevation, P-selectin expression, fibrinogen binding, shape change and aggregation. We also investigated the *in vitro* inhibitory effects of YM-254890 on high-shear stress-induced platelet aggregation (SIPA) in a cone-and-plate viscometer and platelet-rich thrombus formation on a collagen surface under high-shear flow conditions in a parallel-plate flow chamber. The *in vivo* antithrombotic effect of YM-254890 was also evaluated in a model of cyclic flow reductions (CFRs) in the femoral artery of cynomolgus monkeys.

Methods

Preparation of platelets

Blood sample were treated with 3.8% sodium citrate at a rate of 10% ($v\,v^{-1}$) to prevent coagulation and centrifuged at $160 \times g$ for 10 min to obtain platelet-rich plasma (PRP). The PRP was collected, and the whole blood samples were centrifuged again at $1800 \times g$ for 10 min to obtain platelet-poor plasma (PPP). Platelet counts in PRP were determined with an automatic cell counter (MEK-6258; Nihon Kohden, Tokyo, Japan), and were adjusted to 3×10^5 platelets μl^{-1} with PPP. Washed platelets were prepared according to the method of Katagiri *et al*. (1990). PRP was mixed with 10 mM citrate and centrifuged at $1000 \times g$ for 10 min. The precipitate was washed twice with Tyrode's-HEPES buffer (137 mM NaCl, 38 mM HEPES, 2.7 mM KCl, 3.7 mM NaH_2PO_4, 0.98 mM $MgSO_4$, 5.6 mM glucose and 0.35% BSA, pH 6.7) containing 2 U ml^{-1} of potato apyrase, and resuspended in Tyrode's-HEPES buffer (pH 7.4). The suspension was adjusted to an appropriate platelet count with Tyrode's-HEPES buffer (pH 7.4).

Measurement of Fura-2-detected intracellular Ca^{2+} changes

Fura-2-acetoxymethyl ester (3 μM) was added to human PRP and the mixture was incubated at 37°C for 45 min. After incubation, platelets were washed twice according to the procedure described above and resuspended in the same buffer at a final concentration of 1×10^5 platelets μl^{-1}. $CaCl_2$ (1 mM) was added just prior to the experiment. After the addition of $CaCl_2$, Fura-2-loaded washed platelets were incubated with either YM-254890 or MRS2179 for 1 min, and the samples were then stimulated with ADP (10 μM). Fura-2 fluorescence was measured using a fluorescence spectrometer (CAF-110, JASCO Co., Tokyo, Japan) at wavelengths of 340 and 380 nm for excitation and 510 nm for emission. Changes in intracellular Ca^{2+} level were monitored using the fura-2 340/380 fluorescence ratio in an arbitrary unit. To obtain the minimum and maximum fluorescences, the samples were treated with 3 mM EGTA or 0.2% TX-100, respectively. The luminescent signal was converted to $[Ca^{2+}]_i$ using a Fura-2-Ca^{2+} dissociation constant of 224 nm as described by Grynkiewicz *et al*. (1985).

P-selectin expression on ADP- or thrombin receptor agonist peptide (TRAP)-stimulated platelets

The diluted citrated human whole blood (1 : 7 dilution) was incubated with the test drug for 10 min at room temperature. The mixture was stimulated with either ADP (5 μM) or TRAP (20 μM). After the samples were gently mixed, they were incubated at room temperature for 10 min. The samples were incubated with saturating concentrations of perdinin chlorophyll protein (PerCP)-conjugated anti-CD42a antibody and phycoerythrin (PE)-conjugated anti-P-selectin antibody for 20 min in the dark at room temperature. For lysing red blood cells and fixation, the samples were mixed with FACS lysing solution (Becton Dickinson, San Jose, CA, U.S.A.) and stored at 4°C in the dark before analysis. Flow cytometry was performed on a FACSCalibur (Becton Dickinson). Fluorescence channels were set on logarithmic scales. A gate was set around the platelet population, and platelet identity was confirmed using the PerCP-conjugated anti-CD42a antibody. More than 10,000 platelets were analyzed within this gate. The percentage of P-selectin-positive platelets was calculated from the following equation: positive cell (%) = number of both CD42a and P-selectin-positive cells/number of CD42a-positive cells $\times$ 100.

Fibrinogen binding to purified GPIIb/IIIa or washed platelets

The binding of biotinylated human fibrinogen to purified GPIIb/IIIa complex was determined as described by Kawasaki *et al*. (1996). Microtiterplate wells were coated with purified GPIIb/IIIa and blocked with BSA. Biotinylated fibrinogen was dispensed into the wells, and then the plates were incubated for 3 h at 37°C. After washing, the bound fibrinogen was quantified using streptavidin-conjugated horseradish peroxidase (1 : 1000 dilution, Amersham-Pharmacia, Piscataway, NJ, U.S.A.) followed by incubation for 1 h at room temperature, washing, and then color generation using the enzyme substrate TMB (BioRad, Hercules, CA, U.S.A.). After stopping the reaction with sulfuric acid, the absorbance was read at 450 nm on a microplate reader (Model 3550, BioRad).

The binding of fluorescein isothiocianate (FITC)-conjugated human fibrinogen to washed human platelets was performed as described in a previous paper (Kawasaki *et al*., 1996). In all, 400 μl of washed platelets (3×10^5 platelets μl^{-1}) were incubated with EDTA (10 mM), test sample and FITC fibrinogen (20 $\mu g\,ml^{-1}$) in the presence or absence of TRAP (10 μM). At 30 min after incubation at room temperature, the platelet suspension mixture was centrifuged for 10 min at 14,000 r.p.m. After removing the supernatant, PBS was added to the pellet and the mixture was centrifuged again. After discarding the supernatant, 2% Triton X-100 was added to lyse the platelets, after which they were placed into 96-well microplates to measure fluorescence with a CytoFluor 2300 fluorescent plate

reader (Millipore, Bedford, MA, U.S.A.). The excitation filter had a bandwidth of 20 nm centered at 485 nm and the emission filter had a bandwidth of 25 nm centered at 530 nm.

Platelet shape change

Platelet shape change in human PRP (3×10^5 platelets μl^{-1}) was determined using an aggregometer (MCM Hema Tracer 212, MC Medical, Tokyo, Japan), which records the decrease in light when it is transmitted through a stirred suspension. During the analysis of platelet shape change, platelet aggregation was inhibited by use of the neutralizing monoclonal anti-GPIIb/IIIa antibody abciximab (50 $\mu g\,ml^{-1}$). At 1 min after the addition of test sample and abciximab to PRP in an aggregometer at 37°C, ADP (10 μM), collagen (3 $\mu g\,ml^{-1}$), TRAP (5 μM), arachidonic acid (0.5 mM), U46619 (1.5 μM) or A23187 (5 μM) was added. The concentrations of agonists at which platelet shape change was clearly observed were determined using platelets from each volunteer. YM-254890 was used at a concentration of 10 μM, at which it showed the complete inhibition of platelet aggregation. Platelet shape change caused a stable decrease of light transmission.

Platelet aggregation studies

Platelet aggregation in human PRP was measured using an aggregometer. For platelet aggregation studies, an appropriate agonist concentration which produced a submaximal response was determined using platelets from each volunteer. Platelet aggregation in PRP (3×10^5 platelets μl^{-1}) was induced by ADP (5 μM), collagen (0.25–0.5 $\mu g\,ml^{-1}$), TRAP (1–5 μM), arachidonic acid (0.75 mM), U46619 (1–3 μM), phorbol 12-myristate 13-acetate (PMA, 1–5 μM) and ristocetin (1.5 $mg\,ml^{-1}$). For platelet aggregation studies using washed platelets, indomethacin (10 μM) was added to washed platelets (3×10^5 platelets μl^{-1}) to exclude the secondary effects of released thromboxane A_2. Platelet aggregation was induced by thapsigargin (2.5–5 μM) or A23187 (2.5–10 μM). Inhibitory activity was calculated by dividing the maximum rate of decrease in absorbance of a mixture containing the test sample by the maximum rate obtained in the presence of buffer alone.

SIPA in cone and plate viscometry

SIPA was performed as described previously (Ikeda *et al*., 1991). A shear stress gradient (0.06–1.08 $mN\,cm^{-2}$) was applied to human PRP (3×10^5 platelets μl^{-1}) containing the test drug. Aggregation was continuously monitored by recording the intensity of the light transmitted through the platelet suspension from the beginning of shear force application. The inhibitory activity was calculated by dividing the maximum rate of decrease in absorbance of a mixture containing the test agent by the maximum rate obtained in the presence of buffer alone.

Thrombus formation on a collagen surface under high-shear rate conditions

The flow chamber used was the rectangular type (the flow path was 2.0 mm wide, 31 mm in length and 0.1 mm in height). Glass cover slips (24 mm × 50 mm, Matsunami Glass Co., Osaka, Japan) were coated with 20 μl of fibrillar type I collagen (1 $mg\,ml^{-1}$), placed in a humid environment at 4°C overnight and rinsed with PBS before perfusion. Platelets were labeled in human whole blood by direct incubation with the fluorescent dye $DioC_6(3)$ (2 μM). Increasing concentrations of YM-254890 (1–100 nM) were incubated with whole blood from a single donor at 37°C for 10 min, then the sample blood was perfused through the chamber by a syringe pump at a constant flow rate of 0.3 $ml\,min^{-1}$, producing a wall shear rate of 1500 s^{-1}. The total volume occupied by thrombi in an area of 53,334 μm^2 (266.67 μm × 200 μm) was estimated from a series of confocal sections taken at 1.5 μm intervals on the *z*-axis (confocal laser scanning microscope, Olympus Co., Tokyo, Japan). Confocal sections were analyzed using commercial software, TRI/3D-Bon (Ratoc System Engineering Co., Tokyo, Japan). This software was used to determine the thrombus volume and three-dimensional images of thrombi derived from the accumulated patterns of fluorescence for each image on a collagen surface.

Femoral artery thrombosis model in cynomolgus monkeys

Cynomolgus monkeys with body weights ranging from 2.95 to 7.40 kg (Hamri Co. Ltd, Ibaraki, Japan) were sedated with ketamine hydrochloride (5 $mg\,kg^{-1}$, i.m.) and then anesthetized with sodium pentobarbital (10 $mg\,kg^{-1}$, i.v.). Additional amounts of pentobarbital were administered as necessary during the course of the experiment to maintain a level plane of anesthesia. The body temperature of each animal was maintained at 38°C using a heating pad. After endotracheal intubation, respiration of room air was controlled using an artificial respirator. For each monkey, a cannula was inserted into the carotid artery, which was used to monitor blood pressure and heart rate. Another cannula was inserted into the jugular vein for drug administration and blood sample collection. The probe of a pulsed Doppler blood flow meter was placed on a femoral artery that had been freed from the surrounding tissue in order to monitor the femoral blood flow. CFRs were induced in the femoral artery through stenosis and injury. In brief, the stenosis was induced by using a 1-0 silk thread to ligate the femoral artery together with a 26-gauge needle. The needle was then immediately withdrawn, leaving a graded stenosis of the femoral artery. The stenosed artery was clamped several times to produce moderate endothelial damage. The accumulation of platelet aggregates was observed as a gradual reduction in blood flow. When blood flow reached its lowest level, the platelet plug was mechanically dislodged and femoral arterial blood flow was restored. After CFRs were consistently formed, the test drugs (saline and YM-254890) were administered intravenously. The dosage (0–10 $\mu g\,kg^{-1}$) was escalated after total occlusion (zero blood flow) of the vessel was observed three times. YM-254890 was injected at the predetermined dose when the time to occlusion was more than five times that of the saline group. Data were expressed as a CFR rating according to modifications of the method by Leadley *et al*. (1995). A rating of '0' indicates that a compound produced no change in the pattern of CFRs. A rating of '1' is assigned when a compound decreases the rate of acute platelet thrombus formation, as evidenced by a mean time to occlusion exceed an amount 1.5 times that of the saline group. A rating of '2' indicates that a compound prevents occlusive thrombus formation, but does not completely block the formation of nonocclusive platelet aggregates. Complete inhibition of platelet thrombus formation, as indicated by the

maintenance of a constant blood flow, is assigned a rating of '3'.

Each blood sample was collected through the cannula into a syringe containing a 1/10 volume of 3.8% sodium citrate at 1 min after test drug administration. *Ex vivo* platelet aggregation was performed as described above. The plasma concentration of YM-254890 was determined as described in a previous paper (Kawasaki *et al*., 2005). PPP was stored at −40°C until plasma concentration was measured. Each plasma sample (100 μl) was diluted with 200 mM KH_2PO_4 (1 ml). In all, 50 μl of YM-254891 (300 nM), a YM-254890 analogue, was added to the solution as an internal standard. The mixture was loaded into a HLB Extraction Plate (Waters Co., Milford, MA, U.S.A.), and eluted with MeOH (yield 96.3%). The concentration of YM-254890 in the MeOH eluate was analyzed using LC/MS (Alliance HT/ZQ (ESI), Waters Co.) on a Cadenza CD-C18 (4.6 × 75 mm, Imtakt Co., Kyoto, Japan) column at a flow rate of 0.7 ml min^{-1} at 30°C. MeOH/H_2O (75 : 25, 0.1% formic acid) was used as the eluent.

Measurement of bleeding time was performed at 1 min after saline and drug administration. A pneumatic cuff for blood pressure measurement was wrapped around the upper arm and inflated to 40 mmHg, and bleeding time was measured on the forearm with Simplate R (Organon Teknika Co., Durham, NC, U.S.A.) by making a uniform incision 5 mm long and 1 mm deep. Blood flowing from these incisions was gently wiped away with filter paper every 30 s. Bleeding time was defined as the time until bleeding stopped.

Agents

YM-254890 (Figure 1, molecular weight = 959) was isolated from the culture broth of strain *Chromobacterium* sp. QS3666 (Taniguchi *et al*., 2003). Fura-2-acetoxymethyl ester was obtained from Dojin Laboratories (Kumamoto, Japan). PerCP-conjugated anti-CD42a (GP IX) antibody was purchased from Becton Dickinson Immunocytometry Systems (San Jose, CA, U.S.A.). PE-conjugated anti-CD62P (P-selectin) antibody and PE-conjugated mouse IgG_1,κ control (negative control) were purchased from BD Biosciences (San Diego, CA, U.S.A.). A $P2Y_1$ receptor antagonist MRS2179 was obtained from Tocris Cookson Inc. (Ballwin, MO, U.S.A.). TRAP (Ser-Phe-Leu-Leu-Arg-Asn-NH_2) and type I collagen (Horm collagen) were obtained from Funakoshi (Tokyo, Japan) and Nycomed (Munich, Germany), respectively. YM337, an anti-GPIIb/IIIa antibody, was previously described (Harder *et al*., 1999). Abciximab (ReoPro®) was purchased from Eli Lilly Nederland B.V. (Nieuwegein, The Netherlands). Other reagents were commercially obtained.

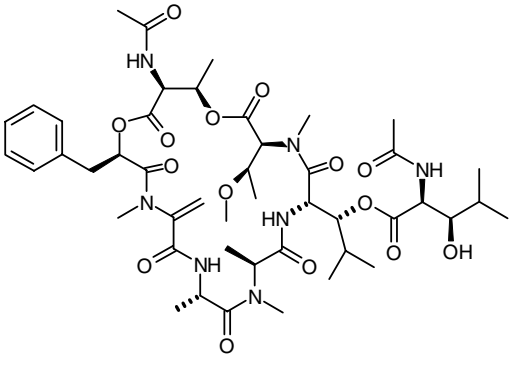

Figure 1 Chemical structure of YM-254890.

Statistical analysis

The experiments, as described elsewhere, were performed at least three times and the data represent the mean ± s.e.m. Statistical analyses for P-selectin expression, fibrinogen binding, thrombus volume, *ex vivo* platelet aggregation, heart rate and mean blood pressure were performed using Dunnett's multiple comparison test or the Student's *t*-test. The statistical analyses of bleeding time for the *in vivo* model of thrombosis were performed using Steel's test. A *P*-value of <0.05 was considered significant.

Results

Intracellular Ca^{2+} elevation

As shown by the tracings in Figure 2, YM-254890 and MRS2179 concentration dependently inhibited intracellular Ca^{2+} elevation induced by ADP, with IC_{50} values of 0.92 ± 0.28 ($n = 3$) and 2.0 ± 1.5 μM ($n = 3$), respectively. In contrast, thapsigargin-induced intracellular Ca^{2+} elevation was unaffected by YM-254890 at 100 μM (data not shown).

P-selectin expression on ADP or TRAP-stimulated platelets

Figure 3 shows the effects of YM-254890 and MRS2179 on P-selectin expression on ADP- (Figure 3a) or TRAP-

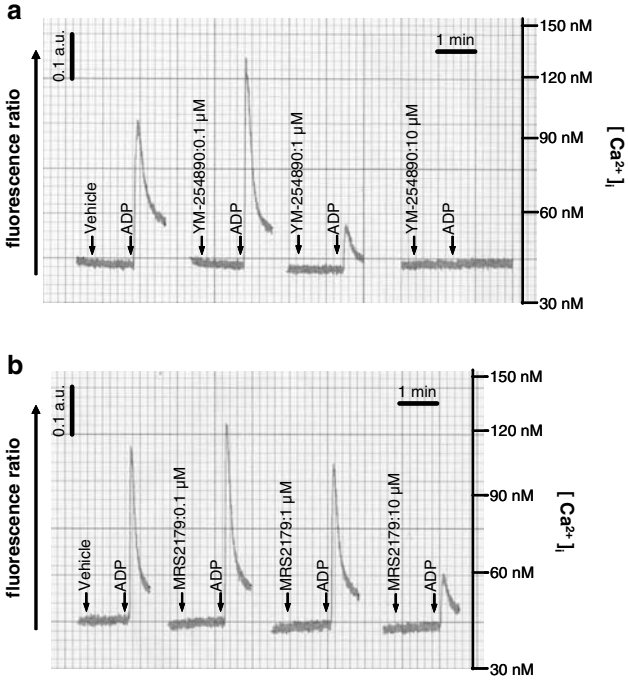

Figure 2 Effects of YM-254890 (a) and MRS2179 (b) on ADP-induced human platelet intracellular Ca^{2+} elevation. Fura-2-loaded platelets were stimulated with ADP (10 μM) 1 min after the addition of test compounds. The data are representative of three separate experiments.

(Figure 3b) stimulated human platelets. For ADP-stimulated platelets, 70±2% of platelets expressed P-selectin ($n=5$), which was significantly higher than for unstimulated platelets (13±1%, $n=5$, $P<0.01$). ADP-induced P-selectin expression was inhibited by YM-254890 and MRS2179 in a concentration-dependent manner, with IC_{50} values of 0.51±0.02 ($n=5$) and 6.4±0.9 μM ($n=5$), respectively. For TRAP-stimulated platelets, 98±1% of platelets expressed P-selectin ($n=5$), which was significantly higher than for unstimulated platelets (7.2±1.7%, $n=5$, $P<0.01$). YM-254890, but not MRS2179, concentration dependently inhibited TRAP-induced P-selectin expression, with an IC_{50} value of 0.16±0.08 μM ($n=5$).

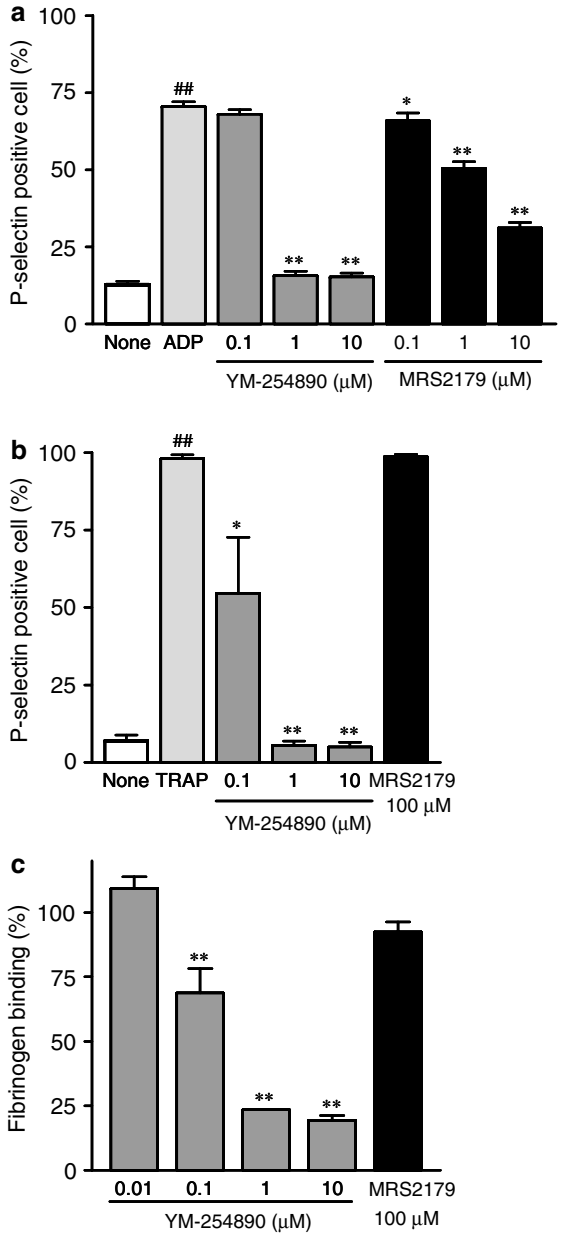

Figure 3 Effects of YM-254890 and MRS2179 on P-selectin expression and fibrinogen binding. P-selectin expression was evaluated in 5 μM ADP- (a) or 20 μM TRAP- (b) stimulated human platelets using flow cytometry. Fibrinogen binding (c) was measured using human PRP stimulated with 20 μM TRAP. Data represent the mean±s.e.m. ($n=3$–5). Statistical analyses were performed using the Student's t-test for comparison with unstimulated platelets or Dunnett's multiple comparison test for comparison with agonist-stimulated platelets. $^{\#\#}P<0.01$ compared with the unstimulated platelets. $^{*}P<0.05$ and $^{**}P<0.01$ compared with the agonist-stimulated platelets.

Fibrinogen binding to purified GPIIb/IIIa or washed platelets

YM-254890 at a concentration of 100 μM had no effect on the binding of biotinylated fibrinogen to purified GPIIb/IIIa (data not shown). In contrast, YM337 concentration dependently inhibited the binding of biotinylated fibrinogen to purified GPIIb/IIIa, with a mean IC_{50} value of 0.16±0.01 μM ($n=3$). Figure 3c shows the effects of YM-254890 and MRS2179 on the binding of fibrinogen to TRAP-stimulated washed human platelets. YM-254890, but not MRS2179, concentration dependently inhibited fibrinogen binding to TRAP-stimulated platelets with an IC_{50} value of 0.47±0.08 μM ($n=3$).

Platelet shape change

Figure 4 shows the representative tracings of human platelet shape change induced by various agonists in the presence or absence of YM-254890. A pronounced shape change was observed after the addition of various agonists, as indicated by an immediate decrease in light transmission. YM-254890 completely inhibited platelet shape change induced by ADP at 10 μM. However, collagen-, TRAP-, arachidonic acid-, U46619- and A23187-induced platelet shape change was not inhibited by YM-254890.

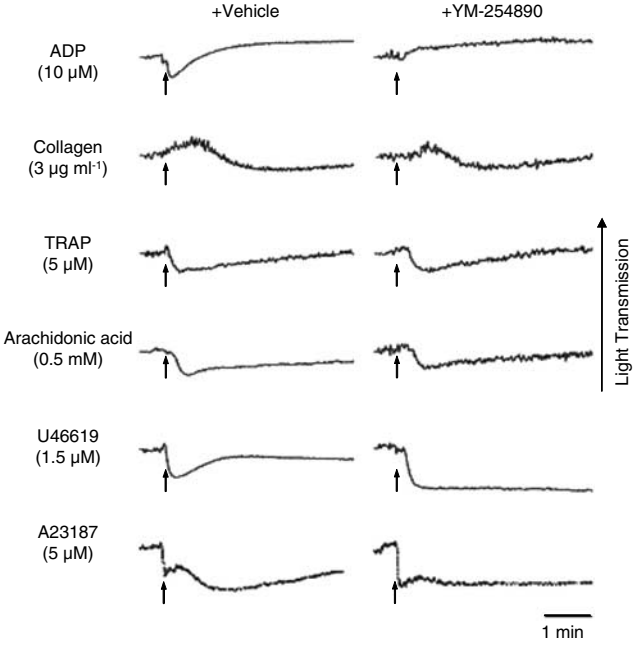

Figure 4 Effect of YM-254890 on human platelet shape change after the addition of various agonists. During the analysis of platelet shape change, platelet aggregation was blocked by the addition of abciximab (50 μg ml^{-1}). At 1 min after the addition of the test sample to PRP in an aggregometer at 37°C, followed ADP (20 μM), collagen (1 μg ml^{-1}), TRAP (5 μM), arachidonic acid (1.5 mM), U46619 (3 μM) or A23187 (5 μM), as shown with arrows. YM-254890 was used at a final concentration of 10 μM for all agonists. The data are representative of three separate experiments.

Platelet aggregation

Table 1 shows IC_{50} values of YM-254890 for human platelet aggregation induced by ADP, collagen, TRAP, arachidonic acid and U46619. In PRP, YM-254890 concentration dependently inhibited platelet aggregation induced by ADP, collagen, TRAP, arachidonic acid and U46619 with IC_{50} values of 0.39 ± 0.06 ($n=3$), 0.15 ± 0.05 ($n=3$), 0.71 ± 0.23 ($n=3$), 0.25 ± 0.04 ($n=3$) and $0.34 \pm 0.11\,\mu$M ($n=3$), respectively. In collagen-induced platelet aggregation with a higher concentration of collagen (20–40 $\mu g\,ml^{-1}$), however, the inhibitory effect by YM-254890 decreased progressively, which was a condition also observed with MRS2179 (data not shown). Furthermore, YM-254890 had no inhibitory effect on PMA- or ristocetin-induced human platelet aggregation at concentrations of 100 μM. In washed human platelets, thapsigargin- and A23187-induced platelet aggregations were not inhibited by YM-254890 at 100 μM. YM337 potently inhibited platelet aggregation induced by all agonists except ristocetin, with IC_{50} values of 6.8–46 nM (data not shown).

SIPA in cone and plate viscometry

The IC_{50} value of YM-254890 is shown in Table 1. Figure 5 shows the representative tracings of the inhibitory effect of YM-254890 on SIPA in human PRP. YM-254890 inhibited high SIPA concentration dependently with an IC_{50} value of $0.57 \pm 0.07\,\mu$M ($n=3$).

Thrombus formation on a collagen surface under high-shear stress conditions

Figure 6a shows the three-dimensional representations of human platelet thrombi on a collagen surface under a high-shear rate of 1500 s^{-1} in the presence and absence of YM-254890. YM-254890 at a concentration of 100 nM inhibited thrombus formation on the collagen surface by $78 \pm 8\%$. Perfusion experiments are summarized in Figure 6b. YM-254890 concentration dependently inhibited thrombus formation, with a mean IC_{50} value of 25 ± 2 nM ($n=5$).

Table 1 Effect of YM-254890 on platelet aggregation induced by various agonists in human PRP and washed human platelets

Agonist	*IC_{50}* (μM)
PRP	
ADP (5 μM)	0.39 ± 0.06
Collagen (0.25–0.5 $\mu g\,ml^{-1}$)	0.15 ± 0.05
TRAP (1–5 μM)	0.71 ± 0.23
Arachidonic acid (0.75 mM)	0.25 ± 0.04
U46619 (1–3 μM)	0.34 ± 0.11
PMA (1–5 μM)	>100
Ristocetin (1.5 $mg\,ml^{-1}$)	>100
SIPA	0.57 ± 0.07
Washed platelets	
Thapsigargin (2.5–5 μM)	>100
A23187 (2.5–10 μM)	>100

The IC_{50} values were calculated from the concentration–inhibition curves for each experiment. Data represent the mean ± s.e.m. of three or four separate experiments.

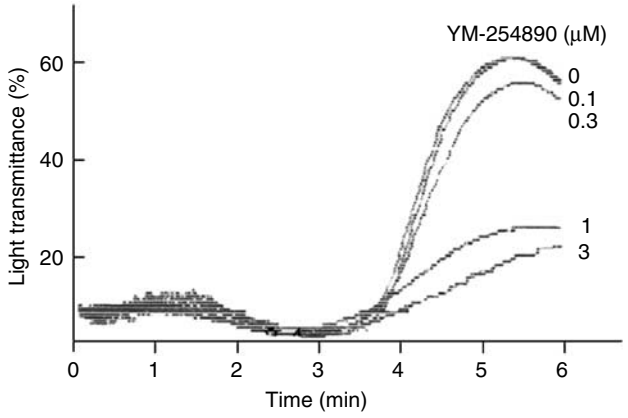

Figure 5 Effect of YM-254890 on SIPA in human PRP. PRP was exposed to a gradient of 6×10^{-5} to 1.08×10^{-3} N cm^{-2} for 6 min at room temperature. After an initial 15 s at 6×10^{-5} N cm^{-2}, the gradient increased from 6×10^{-5} to 1.2×10^{-4} N cm^{-2} over 90 s, from 1.2×10^{-4} to 1.08×10^{-3} N cm^{-2} over the next 120 s, and remained constant at 1.08×10^{-3} N cm^{-2} for the last 135 s. The data are representative of three separate experiments. The YM-254890 concentrations used are indicated.

Femoral artery thrombosis model in cynomolgus monkeys

A typical pattern of femoral arterial mean blood flow is shown in Figure 7a. For the saline group, CFRs occurred in the femoral arteries of all five animals, with a mean occlusion time of 2.0 min. The CFR rating is shown in Figure 7b. YM-254890 dose dependently inhibited platelet thrombus formation, as evidenced by the inhibition of CFRs. Similarly, YM-254890 dose dependently inhibited ADP-induced platelet aggregation, significantly at doses of more than 1 $\mu g\,kg^{-1}$ (Figure 7c). Figure 7d represents the effect of YM-254890 on template bleeding time. The median value of template bleeding time in the saline group was 2 min. At a dose of 10 $\mu g\,kg^{-1}$, YM-254890 tended to prolong bleeding time, but this inclination was not statistically significant ($P=0.053$). Figure 7e shows the relative change in mean BP and HR after an i.v. bolus injection of YM-254890. The basal values of the mean BP and HR were 109 ± 14 mmHg and 153 ± 6 beats min^{-1}, respectively. YM-254890 had no effect on these two parameters at doses up to 3 $\mu g\,kg^{-1}$. At a dose of 10 $\mu g\,kg^{-1}$, the relative change in mean BP and HR was -8.2 ± 2.8 and $3.2 \pm 1.4\%$, respectively, but these changes were not statistically significant ($P=0.14$ and 0.059, respectively). The plasma concentration of YM-254890 was 12, 23 and 104 nM at 1 min after injection at 1, 3 and 10 $\mu g\,kg^{-1}$, respectively, and decreased below the detection limit (<10 ng ml^{-1}) 10 min after administration in the 10 $\mu g\,kg^{-1}$ group. Plasma drug concentration was measured to be below the detection limit in all animals in the 0.1 and 0.3 $\mu g\,kg^{-1}$ groups.

Discussion

In this study, we found that YM-254890 strongly inhibited $G\alpha_q$-mediated intracellular Ca^{2+} elevation, P-selectin expression, fibrinogen binding and platelet aggregation. YM-254890 was also found to produce significant antithrombotic effects not only in the *in vitro* flow chamber assay, but also in a femoral arterial thrombosis model of cynomolgus monkeys.

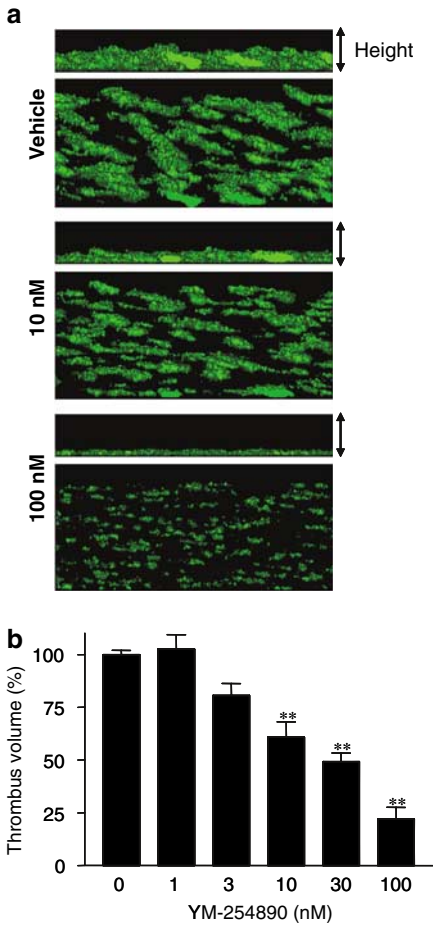

Figure 6 Effect of YM-254890 on human platelet thrombus formation on a collagen surface in a perfusion chamber. (a) Three-dimensional images of platelet thrombus formation on a collagen surface in the presence of YM-254890 under high-shear rate conditions ($1500\,s^{-1}$). The three-dimensional images of thrombus generation on a collagen surface 7 min after the beginning of the perfusion were digitized, and the three-dimensional structures were constructed based on the two-dimensional images using commercial volume analysis software. Top and bottom panels show platelet thrombus images from the horizontal and oblique positions, respectively. (b) The inhibitory effect of YM-254890 on thrombus formation on a collagen surface under high-shear rate conditions. Data are expressed as percent of the thrombus volume formed in the presence of vehicle, and the data represent the mean ± s.e.m. of five separate experiments. Statistical analyses were performed using Dunnett's multiple comparison test for comparison with the vehicle-treated blood samples. $^{**}P<0.01$ compared with the vehicle group.

Phospholipase C (PLC) activation and IP_3 formation through $G\alpha_q$-coupled receptors were shown to be important in calcium elevation from intracellular stores in platelets (Sage *et al*., 2000). Intracellular Ca^{2+} elevation by ADP was strongly inhibited by YM-254890 and MRS2179. Our YM-254890 results correlated well with those obtained from a patient with decreased immunological $G\alpha_q$ (Gabbeta *et al*., 1997) and from $G\alpha_q$-deficient mice (Offermanns *et al*., 1997). MRS2179 results were similar to those found by Baurand *et al*. (2001). Furthermore, thapsigargin-induced Ca^{2+} elevation was unaffected by YM-254890, suggesting that $G\alpha_q$ plays a minor role in mediating the signal generated by Ca^{2+} depletion *via* plasma membrane Ca^{2+}-ATPase activity.

Expression of the P-selectin antigen has increased in patients in a variety of thrombotic/prothrombotic states (Mathur *et al*., 2001; Shebuski & Kilgore, 2002). The expression of P-selectin by ADP- or TRAP-stimulated platelets was strongly inhibited by YM-254890, suggesting that the $G\alpha_q$/PLC-β pathway plays a central role in agonist-induced platelet granule secretion. Similar findings were described for $G\alpha_q$-deficient mice (Offermanns *et al*., 1997). In contrast, MRS2179 inhibited ADP-induced P-selectin expression, but not TRAP-induced P-selectin expression, as described by Janes *et al*. (1994) and Storey *et al*. (2000). These findings also imply that YM-254890 may have a superior benefit to $P2Y_1$ antagonists for the treatment of chronic thrombotic/prothrombotic conditions that involve the release of platelet products.

Agonist-induced conformational changes in the platelet GPIIb/IIIa complex and the resulting fibrinogen binding are essential for platelet aggregation. The binding of biotinylated fibrinogen to purified GPIIb/IIIa was not inhibited by YM-254890, indicating that YM-254890 does not directly act on GPIIb/IIIa receptors. In contrast, the binding of FITC fibrinogen to washed platelets was completely inhibited by YM-254890. These results suggest that signal transduction abnormality leads to the impaired activation of fibrinogen-binding sites. Our results are consistent with those of the activation of GPIIb/IIIa in patients with abnormal pleckstrin phosphorylation and diminished immunoreactive $G\alpha_q$ (Gabbeta *et al*., 1996).

The platelet shape change is due to a fast reorganization of actin filaments (Bearer, 1995). In this study, ADP-induced platelet shape change was completely inhibited by YM-254890, suggesting that this is due to the inhibitory effect of YM-254890 on $G\alpha_q$-mediated PLC-β activation through $P2Y_1$. In contrast, platelet shape change induced by TRAP, collagen, U46619 or A23187 was unaffected by YM-254890, suggesting the existence of $G\alpha_q$-independent platelet shape change pathways. These results are well consistent with those observed in $G\alpha_q$-deficient mice (Offermanns *et al*., 1997). The importance of the $G_{12/13}$-Rho-mediated pathway for TRAP- or U46619-induced platelet shape change and that of the Src/Syk-myosin light chain-kinase pathway for collagen- or A23187-induced platelet shape change have been described elsewhere (Bauer *et al*., 1999).

Platelet aggregation induced by ADP, collagen, TRAP, arachidonic acid and U46619 was completely inhibited by YM-254890, indicating that these agonists activate platelets by $G\alpha_q$-dependent mechanisms. There are, however, $G\alpha_q$-independent signals involved in GPIIb/IIIa activation. The involvement of at least three $G\alpha_q$-independent pathways has been postulated for the induction of the platelet aggregatory response based on experiments using phorbol esters, Ca^{2+}-ATPase inhibitors and Ca^{2+} ionophores. Furthermore, a study of GPIb-vWF modulators indicates that a GPIIb/IIIa-independent pathway is also involved in platelet aggregation (Fujimura *et al*., 1996). The results obtained in this study were consistent with those of Offermanns *et al*. (1997) using $G\alpha_q$-deficient mice. The fact that the inhibitory effect of YM-254890 on platelet aggregation decreased progressively at higher concentrations of collagen suggests that $G\alpha_q$-independent PLC-γ signaling is not disturbed.

vWF-mediated platelet aggregation occurs when shear stress is applied to platelets in the absence of any exogenous agonists (Peterson *et al*., 1987). SIPA at high-shear stress levels appears to be clinically important because these conditions are very likely to be generated in the stenosed coronary artery *in vivo* (Goto *et al*., 1992) In this study, YM-254890 inhibited

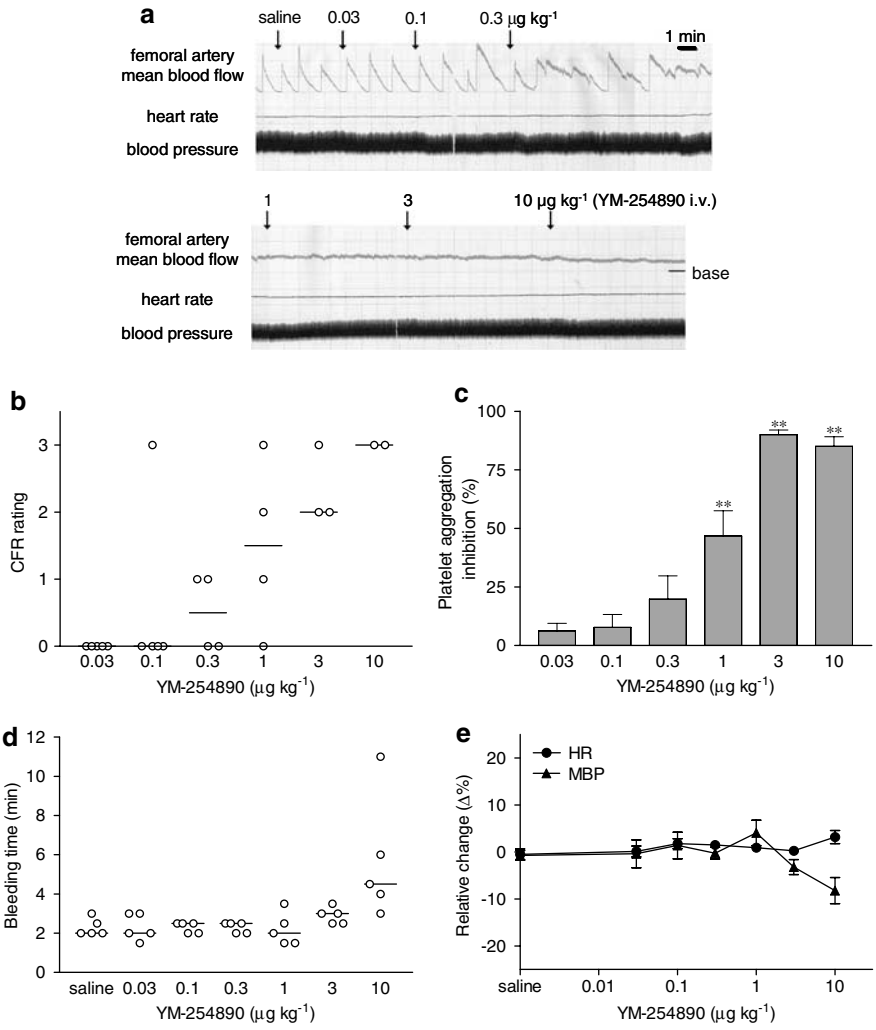

Figure 7 The femoral artery thrombosis model in cynomolgus monkeys. (a) Typical patterns of CFRs, HR and BP after i.v. bolus injection of saline and YM-254890. CFRs were induced in the femoral artery by stenosis and injury. (b) Effect of YM-254890 on platelet thrombus formation. Open circles represent the CFR rating on a scale of 0–3, with 0 indicating no inhibition and 3 indicating complete inhibition. Bars indicate the median values for each dose. (c) Effect of YM-254890 on *ex vivo* ADP-induced platelet aggregation. Data are expressed as the mean ± s.e.m. of five animals. Statistical analysis was performed using Dunnett's multiple comparison test. $^{**}P<0.01$ compared with the saline group. (d) Effect of YM-254890 on bleeding time. Open circles represent the bleeding time for each animal. Bars indicate the median values for each dose. Statistical analysis was performed using Steel's test. (e) Effect of YM-254890 on relative change in HR (closed circles) and BP (closed triangles). Data are expressed as the mean ± s.e.m. of five animals. Statistical analysis was performed using Dunnett's multiple comparison test.

high-SIPA at the same potency as agonist-induced platelet aggregations, indicating the importance of $G\alpha_q$-mediated signal transduction for high-SIPA.

In thrombus formation on a collagen surface under high-shear conditions, the initial interaction of vWF immobilized on a surface with GPIb/IX and subsequent vWF binding to GPIIb/IIIa is indispensable for proper mural thrombus growth (Moroi *et al*., 1996; Tsuji *et al*., 1999). In this study, YM-254890 inhibited platelet thrombus formation on a collagen surface under high-shear rate conditions in a flow chamber more potently than high-SIPA in a cone-and-plate viscometer, suggesting the greater importance of $G\alpha_q$-mediated signal transduction for platelet thrombus growth on a collagen surface under high-shear rate conditions.

In the *in vivo* thrombosis studies using cynomolgus monkeys, YM-254890 exerted antithrombotic effects without any significant prolongation of bleeding time. Its antithrombotic effects were well correlated with those seen in the *ex vivo* inhibition of ADP-induced platelet aggregation and also as observed in another thrombosis model (Kawasaki *et al*., 2003). However, plasma concentrations of YM-254890 were very low even when it exerted effective antithrombotic effects. The reason for this remains unknown, but further pharmacokinetic studies of this compound may explain these apparently inconsistent results. Although systemic hypotension should be cautioned against because of the inhibition of vascular $G\alpha_{q/11}$-coupled signaling (Keys *et al*., 2002), it was noted that no significant hypotension was observed, even at $10\,\mu g\,kg^{-1}$, the dose that completely abolished CFRs in this model. These findings suggest that YM-254890 is a useful antithrombotic agent for patients with high-shear stress-mediated thromboembolic diseases.

In conclusion, YM-254890 potently inhibits $G\alpha_q$-mediated platelet functions and platelet thrombus formation under

high-shear stress conditions. Further studies using this unique compound should lead to a better understanding of the biological functions of $G\alpha_q$-mediated signal pathways.

We thank Marc Hoylaerts for his kind and helpful advice. We are grateful to Koji Nagai, Shigeo Fujita, Shin-ichi Tsukamoto and Isao Yanagisawa for their interest and encouragement.

References

AKKERMAN, J.W. & VAN WILLIGEN, G. (1996). Platelet activation via trimeric GTP-binding proteins. *Haemostasis,* **26,** 199–209.

BAUER, M., RETZER, M., WILDE, J.I., MASCHBERGER, P., ESSLER, M., AEPFELBACHER, M., WATSON, S.P. & SIESS, W. (1999). Dichotomous regulation of myosin phosphorylation and shape change by Rho-kinase and calcium in intact human platelets. *Blood,* **94,** 1665–1672.

BAURAND, A., RABOISSON, P., FREUND, M., LEON, C., CAZENAVE, J.P., BOURGUIGNON, J.J. & GACHET, C. (2001). Inhibition of platelet function by administration of MRS2179, a P2Y1 receptor antagonist. *Eur. J. Pharmacol.,* **412,** 213–221.

BEARER, E.L. (1995). Cytoskeletal domains in the activated platelet. *Cell Motil. Cytoskeleton,* **30,** 50–66.

BIRNBAUMER, L. (1992). Receptor-to-effector signaling through G proteins: roles for beta gamma dimers as well as alpha subunits. *Cell,* **71,** 1069–1072.

BRASS, L.F., HOXIE, J.A. & MANNING, D.R. (1993). Signaling through G proteins and G protein-coupled receptors during platelet activation. *Thromb. Haemost.,* **70,** 217–223.

CLAPHAM, D.E. & NEER, E.J. (1993). New roles for G-protein beta gamma-dimers in transmembrane signalling. *Nature,* **365,** 403–406.

FUJIMURA, Y., KAWASAKI, T. & TITANI, K. (1996). Snake venom proteins modulating the interaction between von Willebrand factor and platelet glycoprotein Ib. *Thromb. Haemost.,* **76,** 633–639.

GABBETA, J., YANG, X., SUN, L., MCLANE, M.A., NIEWIAROWSKI, S. & RAO, A.K. (1996). Abnormal inside-out signal transduction-dependent activation of glycoprotein IIb-IIIa in a patient with impaired pleckstrin phosphorylation. *Blood,* **87,** 1368–1376.

GABBETA, J., YANG, X., KOWALSKA, M.A., SUN, L., DHANASE-KARAN, N. & RAO, A.K. (1997). Platelet signal transduction defect with Galpha subunit dysfunction and diminished Galphaq in a patient with abnormal platelet responses. *Proc. Natl. Acad. Sci. U.S.A.,* **94,** 8750–8755.

GOLDSCHMIDT, P.J., LOPES, N. & CRAWFORD, L.E. (2002). Atherosclerosis and coronary artery diseases. In: *Platelet*. ed. Michelson A.D., pp. 375–398. CA: Elsevier/U.S.A..

GOTO, S., IKEDA, Y., MURATA, M., HANDA, M., TAKAHASHI, E., YOSHIOKA, A., FUJIMURA, Y., FUKUYAMA, M., HANDA, S. & OGAWA, S. (1992). Epinephrine augments von Willebrand factor-dependent shear-induced platelet aggregation. *Circulation,* **86,** 1859–1863.

GRYNKIEWICZ, G., POENIE, M. & TSIEN, R.Y. (1985). A new generation of Ca^{2+} indicators with greatly improved fluorescence properties. *J. Biol. Chem.,* **260,** 3440–3450.

HARDER, S., KIRCHMAIER, C.M., KRZYWANEK, H.J., WESTRUP, D., BAE, J.W. & BREDDIN, H.K. (1999). Pharmacokinetics and pharmacodynamic effects of a new antibody glycoprotein IIb/IIIa inhibitor (YM337) in healthy subjects. *Circulation,* **100,** 1175–1181.

IKEDA, Y., HANDA, M., KAWANO, K., KAMATA, T., MURATA, M., ARAKI, Y., ANBO, H., KAWAI, Y., WATANABE, K., ITAGAKI, I., SAKAI, K. & RUGGERI, Z.M. (1991). The role of von Willebrand factor and fibrinogen in platelet aggregation under varying shear stress. *J. Clin. Invest.,* **87,** 1234–1240.

JANES, S.L., WILSON, D.J., COX, A.D., CHRONOS, N.A. & GOODALL, A.H. (1994). ADP causes partial degranulation of platelets in the absence of aggregation. *Br. J. Haematol.,* **86,** 568–573.

KATAGIRI, Y., HAYASHI, Y., YAMAMOTO, K., TANOUE, K., KOSAKI, G. & YAMAZAKI, H. (1990). Localization of von Willebrand factor and thrombin-interactive domains on human platelet glycoprotein Ib. *Thromb. Haemost.,* **63,** 122–126.

KAWASAKI, T., SAKAI, Y., TANIUCHI, Y., SATO, K., MARUYAMA, K., SHIMIZU, M., KAKU, S., YANO, S., INAGAKI, O., TOMIOKA, K., YANAGISAWA, I. & TAKENAKA, T. (1996). Biochemical characterization of a new disintegrin, flavostatin, isolated from *Trimeresurus flavoviridis* venom. *Biochimie,* **78,** 245–252.

KAWASAKI, T., TANIGUCHI, M., MORITANI, Y., HAYASHI, K., SAITO, T., TAKASAKI, J., NAGAI, K., INAGAKI, O. & SHIKAMA, H. (2003). Antithrombotic and thrombolytic efficacy of YM-254890, a Gq/11 inhibitor, in a rat model of arterial thrombosis. *Thromb. Haemost.,* **90,** 406–413.

KAWASAKI, T., TANIGUCHI, M., MORITANI, Y., UEMURA, T., SHIGENAGA, T., TAKAMATSU, H., HAYASHI, K., TAKASAKI, J., SAITO, T. & NAGAI, K. (2005). Pharmacological properties of YM-254890, a specific $G\alpha_{q/11}$ inhibitor, on thrombosis and neointima formation in mice. *Thromb. Haemost.,* **94,** 184–192.

KEYS, J.R., GREENE, E.A. & KOCH, W.J. (2002). G_q-coupled receptor agonists mediate cardiac hypertrophy via the vasculature. *Hypertension,* **40,** 660–666.

LEADLEY JR, R.J., HUMPHREY, W.R., ERICKSON, L.A. & SHEBUSKI, R.J. (1995). Inhibition of thrombus formation by endothelin-1 in canine models of arterial thrombosis. *Thromb. Haemost.,* **74,** 1583–1590.

MATHUR, A., ROBINSON, M.S., COTTON, J., MARTIN, J.F. & ERUSALIMSKY, J.D. (2001). Platelet reactivity in acute coronary syndromes: evidence for differences in platelet behaviour between unstable angina and myocardial infarction. *Thromb. Haemost.,* **85,** 989–994.

MOROI, M., JUNG, S.M., SHINMYOZU, K., TOMIYAMA, Y., ORDINAS, A. & DIAZ-RICART, M. (1996). Analysis of platelet adhesion to a collagen-coated surface under flow conditions: the involvement of glycoprotein VI in the platelet adhesion. *Blood,* **88,** 2081–2092.

OFFERMANNS, S. (2000). The role of heterotrimeric G proteins in platelet activation. *Biol. Chem.,* **381,** 389–396.

OFFERMANNS, S., TOOMBS, C.F., HU, Y.H. & SIMON, M.I. (1997). Defective platelet activation in G alpha(q)-deficient mice. *Nature,* **389,** 183–186.

PETERSON, D.M., STATHOPOULOS, N.A., GIORGIO, T.D., HELLUMS, J.D. & MOAKE, J.L. (1987). Shear-induced platelet aggregation requires von Willebrand factor and platelet membrane glycoproteins Ib and IIb-IIIa. *Blood,* **69,** 625–628.

SAGE, S.O., YAMOAH, E.H. & HEEMSKERK, J.W. (2000). The roles of P2X1 and P2TAC receptors in ADP-evoked calcium signalling in human platelets. *Cell Calcium,* **28,** 119–126.

SHEBUSKI, R.J. & KILGORE, K.S. (2002). Role of inflammatory mediators in thrombogenesis. *J. Pharmacol. Exp. Ther.,* **300,** 729–735.

STOREY, R.F., SANDERSON, H.M., WHITE, A.E., MAY, J.A., CAMERON, K.E. & HEPTINSTALL, S. (2000). The central role of the P(2T) receptor in amplification of human platelet activation, aggregation, secretion and procoagulant activity. *Br. J. Haematol.,* **110,** 925–934.

TAKASAKI, J., SAITO, T., TANIGUCHI, M., KAWASAKI, T., MORITANI, Y., HAYASHI, K. & KOBORI, M. (2004). A novel $G\alpha_{q/11}$-selective inhibitor. *J. Biol. Chem.,* **279,** 47438–47445.

TANIGUCHI, M., NAGAI, K., ARAO, N., KAWASAKI, T., SAITO, T., MORITANI, Y., TAKASAKI, J., HAYASHI, K., FUJITA, S., SUZUKI, K. & TSUKAMOTO, S. (2003). YM-254890, a novel platelet aggregation inhibitor produced by *Chromobacterium* sp. QS3666. *J. Antibiot.,* **15,** 358–363.

TSUJI, S., SUGIMOTO, M., MIYATA, S., KUWAHARA, M., KINOSHITA, S. & YOSHIOKA, A. (1999). Real-time analysis of mural thrombus formation in various platelet aggregation disorders: distinct shear-dependent roles of platelet receptors and adhesive proteins under flow. *Blood,* **94,** 968–975.

(Received July 15, 2005
Revised November 8, 2005
Accepted January 26, 2006
Published online 6 March 2006)